

# We are IntechOpen, the world's leading publisher of Open Access books Built by scientists, for scientists

6,900

Open access books available

186,000

International authors and editors

200M

Downloads

Our authors are among the

154

Countries delivered to

TOP 1%

most cited scientists

12.2%

Contributors from top 500 universities



WEB OF SCIENCE™

Selection of our books indexed in the Book Citation Index  
in Web of Science™ Core Collection (BKCI)

Interested in publishing with us?  
Contact [book.department@intechopen.com](mailto:book.department@intechopen.com)

Numbers displayed above are based on latest data collected.  
For more information visit [www.intechopen.com](http://www.intechopen.com)



# Role of Heat Transfer on Process Characteristics During Electrical Discharge Machining

Ahsan Ali Khan

*International Islamic University Malaysia  
Malaysia*

## 1. Introduction

Different non-traditional machining techniques are getting more and more employed in manufacturing of complex machine components. Among the non-traditional methods of material removal processes, electrical discharge machining (*EDM*) has drawn a great deal of researchers' attention because of its broad industrial applications (Zarepour, et al., 2007).

In this process material is removed by controlled erosion through a series of electric sparks between the tool (electrode) and the workpiece (Ghosh & Malik, 1991). The sparks are conducted in a dielectric medium. During the spark discharge the dielectric material is ionized and allows the electrons to pass, but it should be deionized immediately after the spark. In the present study kerosene was used as the dielectric medium. The sparks leads to intense heat conductions onto workpiece causing melting and vaporizing of workpiece material (Yan & Tsai, 2005). The temperature during *EDM* may rise from 8000 °C to 20,000 °C. This high heat energy can melt almost any material. *EDM* has become one of the most widely used non-traditional machining processes and can be used on any material that conducts electricity. *EDM* is widely used in machining high strength steel, tungsten carbide and hardened steel (Wang & Tsai, 2001). These materials are used in making dies and molds and it is very difficult to machine them by conventional metal cutting techniques. Fig. 1 shows that die-sinking applications are typically dominated by plastic injection and various other mold fabrications processes.

*EDM* may be used to cut and shape hard materials and complex shapes but can cause surface damage as the electrical charge flows between the electrode and workpiece material. Because there is no mechanical contact between the tool and the workpiece as in traditional operation, the hardness, toughness and strength of the workpiece material has minimal effect on the material removal rate (*MRR*).

*EDM* is gaining popularity due to the following reasons:

**Machining of Complex Shapes:** Complex cavities can often be machined without difficulties by *EDM*. It can be used to machine material with small or odd shaped holes, a large number of holes, holes having shallow entrance angles, intricate cavities, or intricate contour.

**Adaptability to Micro-Machining:** Micro-*EDM* has been adopted as one of the most valuable techniques for micro-fabrication. Micro- *EDM* is accepted as an efficient method for the

fabrication of precise micro-metal components and holes because of its excellence minimum machinable size and diameters of about  $5\ \mu\text{m}$ . *EDM* is the only process capable of machining three dimensional micro workpiece of size as small as  $0.01\ \text{mm}$ . With development of the technology micro workpieces find their applications in micro electro mechanical systems (MEMS).

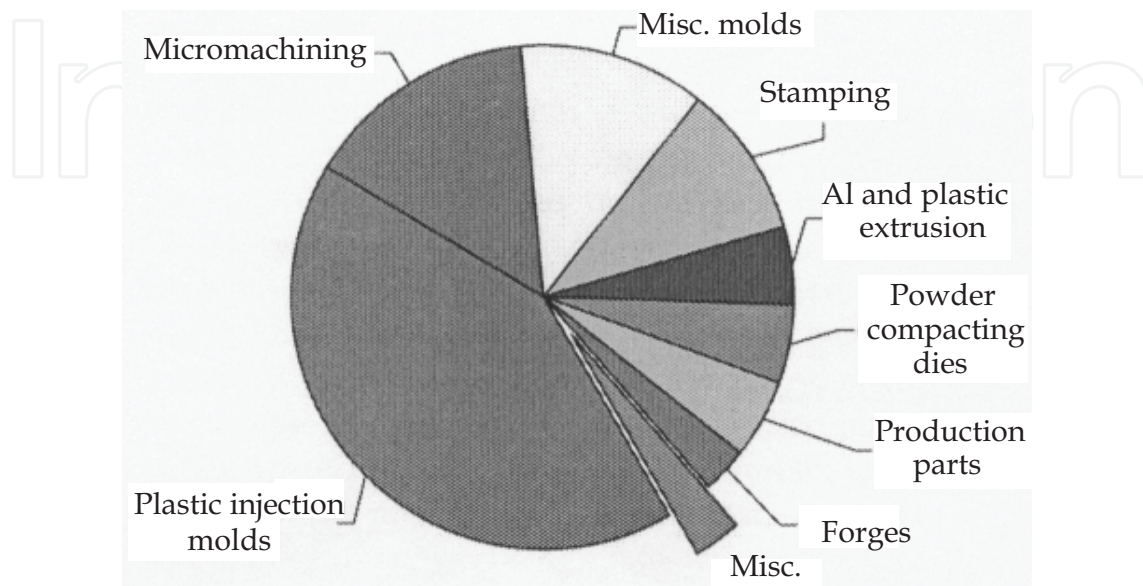


Fig. 1. Application of EDM die-sinking (Peter Fonda et al., 2007)

**High Degree of Automation:** The high degree of automation and the use of tool and workpiece changers allow the machines to work unattended for overnight or during the weekends. CNC control with feedback is generally used and the automatic electrode and pallet changers can be added to *EDM* machine; thus, the process lends itself to unattended and safe operation.

**Accuracy of the Process:** *EDM* is a very accurate machining process. Especially in the case of wire-*EDM*, where the electrode (wire) is constantly renewed with the continuous unwinding of the wire (no effect of tool wear and other tool inaccuracies), very accurate structures can be machined. In the case of workpiece with a higher thickness, the accuracy and the fine surface quality remains the same over the whole thickness of the workpiece, due to the fact that the *EDM* wire is machining with the same process conditions over the total workpiece height (Ho and Newman, 2003).

**Insensitive to the Hardness of the Material (Workpiece):** The capability of machining hard materials is one of the main advantages of *EDM*, as most of the tools for forging, extrusion, die-casting dies and moulds are made of hard materials to increase their lifetime. The recent developments in cutting tools for turning and milling and the processes of high speed machining allow to machine harder materials than before, but *EDM* still remains the only available process for machining many hard materials. One of the important areas of *EDM* application is in mould and dies making industries. To have a mould with longer life span, workpiece material must be very hard. The high hardness of the workpiece is usually obtained by a heat treatment. After the treatment, most workpiece cannot be machined by conventional processes; *EDM* is the appropriate technique to manufacture these workpiece.

Absence of mechanical forces on the workpiece: The EDM-process is based on a thermal principle; no mechanical force is applied to the workpiece; it eliminates the mechanical stresses, chatter and vibration problem during machining (Ho and Newman, 2003). This allows the effective machining of very thin, delicate and fragile workpiece without distortion. The large cutting force of the materials removal processes on the convectional machines is absent in EDM.

The electrode is the main part of the EDM process, which is connected to the DC power source and is immersed in the dielectric fluid. The two main types of electrode materials are copper and graphite. Each of these materials has their own important and distinguishing features. Graphite is a widely used electrode material, but unlike most metals it does not melt but undergoes sublimation at around 3350°C. This is the reason why graphite shows less wear than copper, as there is less thermal damage. Graphite also has superior fabrication capabilities. Other materials used for making electrodes are brass, copper-tungsten, tungsten carbide, zinc, aluminum, etc. (Kalpakjian 2001; Zaw, 1999). Efforts have been done to minimize electrode wear (*EW*). A metal matrix composite ( $ZrB_2$ -Cu) was developed adding different amount of Cu to get an optimum combination of wear resistance, electrical and thermal conductivity of electrodes (Khanra et al., 2007). It was reported that  $ZrB_2$ -40 wt% Cu composite shows more *MRR* with less *EW*. The electrode material is to be selected carefully depending on the work material to machine. The main important properties of electrode materials are electrical conductivity and thermal conductivity. During EDM, the main output parameters are *MRR*, *EW*, wear ratio (*WR*) and job surface finish (*Ra*) (Marafona & Wykes, 2000; Wang & Tsai, 2001). The suitability of the electrodes is judged considering the machining output parameters. *EW* is quite similar to the material removal mechanism as the electrode and the workpiece are considered as a set of electrodes in EDM (Ho & Newman, 2003). Due to this wear, electrodes lose their dimensions resulting inaccuracy of the cavities formed (Khan & Mridha, 2006). Research works have been conducted to draw the relationship of *MRR* with current, voltage, pulse duration, etc (Ramasawmy & Blunt, 2001). C. F. Hu et al., 2008 found that *MRR* was enhanced acceleratively with increasing discharge current and work voltage, but increased deceleratively with pulse duration. Manufacturing of electrodes of special composition is expensive and not always cost effective. In order to maintain the accuracy of machining, *EW* compensation has been reported to be an effective technique, where wear was continuously evaluated by sensors and the compensation was made (Bleys et al., 2004). Some researchers have tried to develop mathematical models to optimize the *EW* and *MRR* (Puertas et al., 2004; Kunieda et al., 2004). It was reported that *MRR* can be substantially increased with reduced *EW* using a multi-electrode discharging system. But again, a special electrode involves additional cost. In the present study the most common and easily available electrode materials like copper and brass were taken under consideration during machining of aluminum and mild steel. Wear of the electrode along the direction of movement of the electrode can be compensated by imparting additional movement of the electrode. But the wear along the cross-section of the electrode cannot be compensated. This phenomenon results inaccuracy in the dimension of the cavities made by die-sinking technique of EDM. In the present study an analysis has been done to evaluate the *EW* along the cross-section of the electrode compared to the same along its movement. An analysis has also been done on the comparative performance of copper and aluminum as electrode materials.

## 2. Heat source models

A number of different heat input methods have been adopted by various researchers to predict the temperature distribution in electrodes. One of the models is disk heat source used to simulate heat input into the workpiece surface. The heat source was insulated at the outer area and assumed to exist during the pulse on-time. The authors assumed that the fraction of the energy transferred to the workpiece is 50%. Tariq & Pandey, 1984 developed models assuming that the heat from the plasma channel is transferred to the workpiece or electrode by conduction only. About 90% of the total energy liberated is conducted to the discharge gap and it was distributed equally between the electrode and workpiece. DiBitonto et al, 1989 approximated the heat source by a point instead of a disk for conducting heat to the interior. The point heat source can result in pulse with high current density and a very small hot spot on the electrode. Uniformly distributed heat source within the spark was considered by most EDM researchers, this assumption is not in line with real EDM process (Vinod Yadav et al., 2002). This point is buttressed by the actual craters shape formed during EDM. Gaussian heat input model gives the best approximation of EDM plasma shape, which accounts for its wide usage by EDM researchers. This is evident by the works of Marafona & Chousal, 2006.

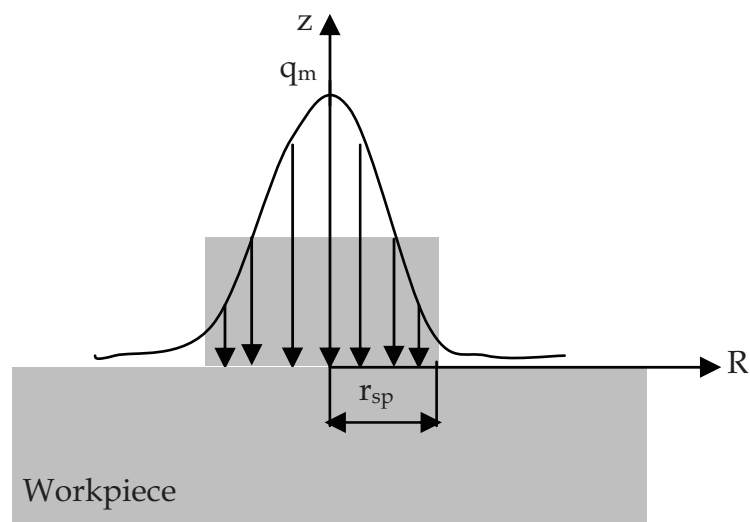


Fig. 2. Gaussian heat source model

For a Gaussian heat distribution, if the maximum heat intensity  $q_m$  (Fig. 2) is at the axis of a spark and its radius ( $r_{sp}$ ) are known, the heat flux  $q_f$  at radius  $R$  is given by:

$$\text{Heat flux } q_f(R) = \frac{4.45 W_M I V}{\pi (r_{sp})^2} \times e^{\left[ -4.5 \left( \frac{R}{r_{sp}} \right)^2 \right]} \quad (1)$$

where

$q_f$  = Heat flux (W/ mm<sup>2</sup>);  $W_M$  = Fraction of energy utilized by the material (Watt)

$I$  = Pulse current (Amp);  $V$  = Gap voltage (Volt)

$R$  = Radial distance from the axis of the spark ( $\mu\text{m}$ );  $r_{sp}$  = Plasma channel radius ( $\mu\text{m}$ )

## 2.1 Plasma channel radius

The extreme high temperature gradient that exists between plasma channel and electrode-workpiece interface enhances heat conduction through the contact surface. Plasma channel with high-energy plasma exhibits spatial and sequential variation at plasma channel-electrode-workpiece interface. This leads to variation in energy flux available for conduction into the electrode and workpiece (Dibitonto et al., 1989). Plasma channel radius is proportional to current, pulse duration, and the proportionality constants and indices depend on inter-electrode gap, electrode and workpiece materials and as well as dielectric fluid (Marafona & Chousal, 2006).

Measurement of plasma channel radius is extremely difficult due to very high pulse frequencies (Vinod Yadav et al., 2002). There are number of different equations used to calculate plasma channel radius according to different authors. It was proposed to use Eq 2 which depends on discharge current and time to calculate plasma channel radius.

$$R(t) = KQ^m t^n \quad (2)$$

where

$R$  = Plasma channel radius ( $\mu\text{m}$ )

$Q$  = Discharge current (Amp)

exponents  $m$ ,  $n$  and  $K$  are empirical constant

Eq. 3 obtained by Patel et al, 1989 was used to calculate plasma channel radius in EDM process. According to the authors, the equation is time dependent with the empirical constants  $K$  and exponent  $n$  given as 0.788 and 0.75 respectively

$$R(t) = K t^n \quad (3)$$

In the work of Shuvra et al, 2003 it was pointed out that plasma radius varies with time as per the relationship in Eq. 4

$$a = R t^{\frac{3}{4}} \quad (4)$$

where  $t$  is time in  $\mu\text{s}$ ,  $a$  is radius in  $\mu\text{m}$  and  $R$  is the proportionality constant.

According to Shuvra et al, because they could not have a good estimated value of proportionality constant  $R$ , they took plasma radius ( $a$ ) to be 0.75  $\mu\text{m}$  which is equal to the radius of the crater. Pandey & Jilani, 1986 in their paper titled, "Plasma channel growth and the resolidified layer in EDM", used Eq. 5 to calculate the plasma radius  $R$ .

$$T_b = \frac{E_o R}{K \pi^{0.5}} \tan^{-1} \left[ \frac{4 a t}{R^2} \right]^{0.5} \quad (5)$$

where  $T_b$  = boiling temperature ( $^{\circ}\text{C}$ ),  $E_o$  is the energy density (Watt/  $\text{m}^2$ ) and  $a$  is the thermal diffusivity ( $\text{m}^2/\text{s}$ ). Salonitis et al, 2007 in their works used Eq. 6 to obtained equivalent heat input radius which is dependent on the current intensity and pulse on-time duration.

$$r_{sp} = 2040 \times (I)^{0.43} \times (t_{on})^{0.44} \quad (6)$$

where  $r_{sp}$  is heat input radius in  $\mu\text{m}$ ,  $I$  is current intensity in A and  $t_{on}$  is the spark time in  $\mu\text{s}$ . In the work of Bulent et al., 2006 and Ozgedik & Cogun, 2006 they used Eq. 7 to estimate the energy released due to a single spark.

$$E_{sp} = I \times V \times t_{on} \quad (7)$$

where

$E_{sp}$  = Energy released due to one spark (Watt)

$I$  = Pulse current (Amp)

$V$  = Gap voltage (Volt)

$t_{on}$  = on-time ( $\mu\text{s}$ )

According to Bulent Ekmekci et al, 2006 the total energy received by any material due to a single spark depends on its thermal conductivity, and is given by Eq. 8.

$$E_M = W_M \times I \times V \times t_{on} \quad (8)$$

where

$E_M$  = Total energy received by the material (Watt)

$W_M$  = Fraction of energy received by the material (Watt)

### 3. Experimental details

#### 3.1 Electrode and work materials

In the present study copper and brass were taken as the electrode materials. These materials have high electrical and thermal conductivity. High electrical conductivity of these materials facilitates conducting electrical sparks. Their high thermal conductivity allows the absorbed heat to escape easily and thus reduces  $EW$ . Moreover, it is easy to machine these materials by conventional machining techniques into complex shapes. The electrodes used in the present study were 70 mm long with a cross-sectional dimension of 15 mm x 15 mm. The major properties of the electrode materials are shown in Table 1.

Electrode materials	Thermal conductivity (W/ m-°K)	Melting point (°C)	Electrical resistivity (ohm-cm)	Specific heat capacity (J g-°C)
Copper	391	1083	1.69	0.385
Brass	159	990	4.7	0.38

Table 1. Major properties of electrode materials

The workpiece materials used in the present study were mild steel and aluminum. Their chemical composition and major properties are shown in the Table 2 and Table 3 respectively.

Work materials	Chemical composition
Aluminum	Al: 99.9%, Cu:0.05%, Fe:0.4%, Mg:0.05%, Mn:0.05%, Si:0.25%, Zn:0.05%
Mild steel	C: 0.14%-0.2%, Fe: 98.81-99.26%, Mn: 0.6%-0.9%, P: 0.04%, S: 0.05%

Table 2. Chemical composition of the work materials

Work materials	Thermal conductivity (W/ m-°K)	Melting point (°C)	Electrical resistivity (ohm-cm)	Specific heat capacity (J g-°C)	Hardness (HB)	Tensile strength (MPa)	Yield strength (MPa)	Percentage elongation at break (%)
Aluminum	227	660	2.9	0.9	35	131	124	8
Mild steel	51.9	1523	1.74	0.472	143	475	275	38

Table 3. Major properties of work materials

### 3.2 EDM machine

The experimental work were conducted on a die sinking EDM machine of type Mitsubishi EX 22 model C11E FP60E. The machine has a rectangular table for mounting the workpiece. The electrode is fixed above the workpiece on the tool holder and can be given a vertical feed to machine a particular cavity. Usually the electrode is connected to the negative terminal and the workpiece is connected to the positive terminal of the power supply which is called direct polarity. However, depending on the combination of the electrode and the work materials, reverse polarity is also sometimes used. The machine used in the present study is shown in Fig. 3.

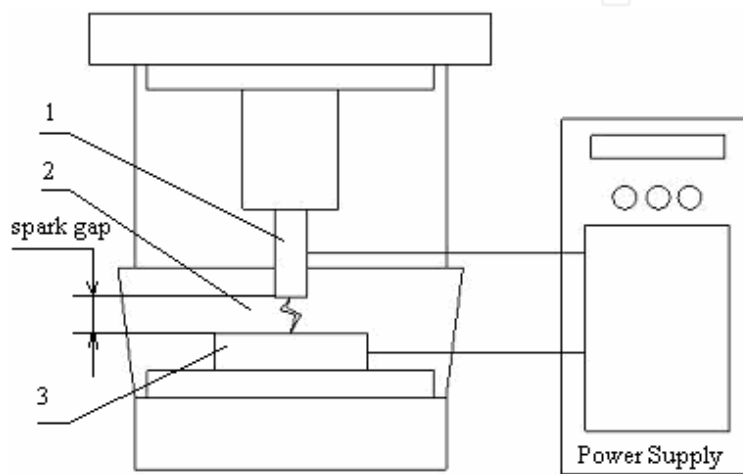


Fig. 3. EDM die sinking machine

### 3.3 Dielectric material

The common properties of dielectric fluids are: The dielectric fluid should have sufficient and stable dielectric strength; it should de-ionize rapidly after the spark discharge; it should have low viscosity and good wetting capacity; its flash point should be sufficient high to avoid any fire hazard; it should not emit any toxic vapours or have unpleasant odours; it should maintain its properties under all working conditions; it should be chemically neutral to the workpiece, electrode or the work table and it should be easily available at a reasonable price. Considering the above factors, kerosene was selected as the dielectric fluid in the present study.

The product of machining, the tiny debris should be removed from the machining zone in order to avoid sparks between the electrode and the debris. This is done by effective flushing system of the dielectric fluid to remove the debris away from the machining zone. Suction flushing of dielectric fluid is preferred when straight vertical walls of the machined cavity are needed. The vertical surfaces are produced with a small taper angle of 0.005mm to 0.05mm per 10mm depth when pressure flushing is employed. However, for machining die cavities a small taper angle is desired. In the present study the machine was incorporated with circulating emission flushing system coupled with jets of three nozzles in order to assure the adequate flushing of the debris from the gap between the tool and the electrode. The experimental set-up is shown in Fig. 4. The current tried in the experiments were 2.5 amps, 3.5 amps and 6.5 amps. The level of voltage used was 10 volts and 5 volts.



1 – tool; 2 – dielectric fluid; 3 – workpiece

Fig. 4. Set-up for the experiments

Square holes of dimensions of 15 mm x 15 mm were machined with a depth of 3 mm. After machining, the wear (Fig. 5) along the direction of the electrode movement (y-direction) and across the electrode (x-direction) was measured using an optical microscope Mitutoyo Hisomet II.

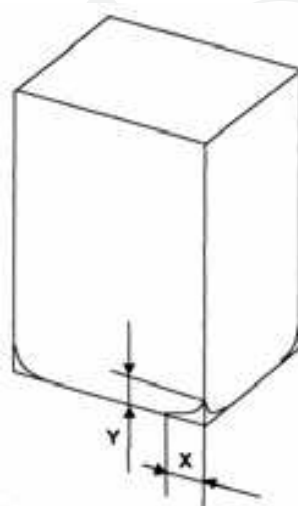


Fig. 5. Electrode wear in x and y directions

## 4. Results and discussions

### 4.1 Electrode wear rate

The present EDM technology allows for a very small level of *EW* because *EW* cannot be eliminated completely. *EW* is a critical problem in EDM since the tool shape degeneration directly affects the final shape of the product. In addition, the cost of a part manufactured by EDM is directly determined by the tool cost, which consists of the raw material cost, the production cost and the number of electrodes required for the machining. In most EDM operations, the cost of the electrode contributes more than 70% to the total operation cost. Due to these reasons, *EW* should be carefully taken into consideration in planning and designing EDM operations. Electrode wear is affected by the precipitation of carbon from the hydrocarbon dielectric onto the electrode surface during sparking. The thickness of the carbon inhibitor layer made a significant improvement on the *EWR* with little effect on the *MRR*.

As it was mentioned before, during EDM the electrode is connected to the negative terminal and the workpiece is connected to the positive terminal of the power supply. Generally, the rate of material removal from the cathode is comparatively less than that from the anode due to the following reasons (Ghosh & Malik, 1991):

- i. The momentum with which the stream of electrons strikes the anode is much more than that due to the stream of the positive ions impinging on the cathode though the mass of an individual electron is less than that of the positive ions.
- ii. The pyrolysis of the dielectric fluid (normally a hydrocarbon) creates a thin film of carbon on the cathode.
- iii. A compressive force is developed on the cathode surface.

Therefore, normally, the tool is connected to the negative terminal of the DC source.

The weight of the electrodes before and after machining gives *EW*. It can be expressed as follows:

$$EWR = \frac{\text{volume of material removed from the electrode}}{\text{machining time}}$$

$$EWR = \frac{EVB - EWA}{MT}$$

where *EVB* and *EWA* are the volumes of the workpiece before and after machining and *MT* is the machining time.

In Fig. 6 to Fig. 9 electrode wear along the cross-sectional direction and along the length of the tool has been presented after a machining a cavity of 3 mm depth. Fig. 6 to Fig. 9 shows that electrode wear rate increases both in x-direction and y-direction with increase in current. It is obvious that a higher current will produce a stronger spark which would cause more material to be eroded from the electrodes. It can also be observed that at a higher gap voltage an electrode undergoes more wear compared to that at a low gap voltage.

For example, during machining of aluminum with brass electrode with a current of 3.5 A the *EW* in x-direction is 0.64 mm at a gap voltage of 5 volts (Fig. 6), whereas, under the same condition the wear in x-direction is 0.86 mm at a gap voltage of 10 volts (Fig. 8).

It can be observed that in all cases (Fig. 6 to Fig. 9) wear of the electrodes in y-direction (along the length) is less than that in x-direction (along the cross-section) of the electrodes. As it was mentioned before, the length of the electrode is 70 mm (in y-direction) and the length of each side of the cross-sectional area is 15 mm (in x-direction). As a result the heat generated during the spark cannot be transferred into the body of the electrode easily in x-direction

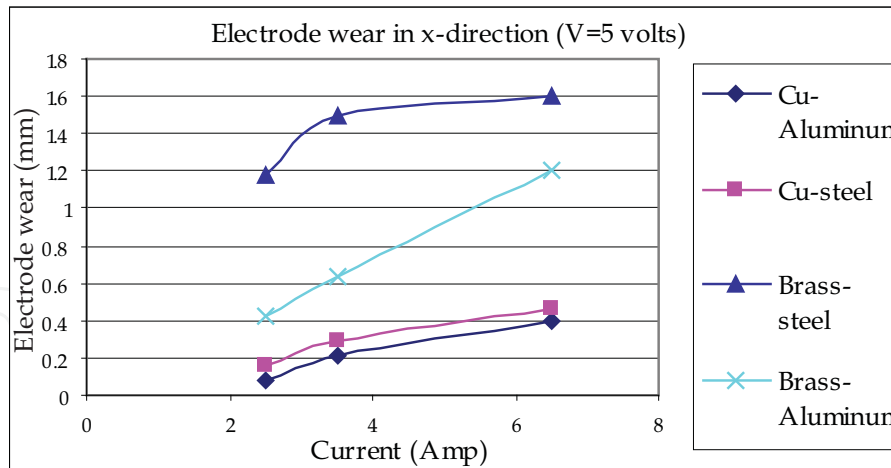


Fig. 6. Relationship of current with electrode wear along the cross-section (v=5 volts)

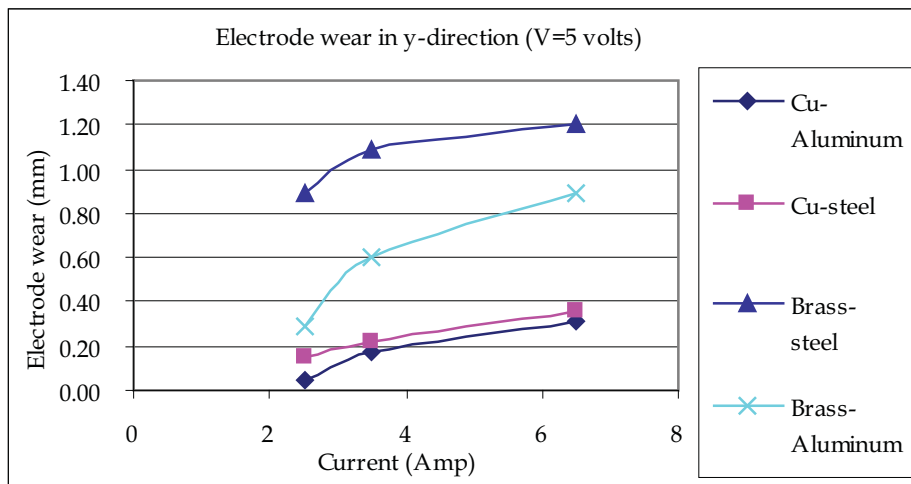


Fig. 7. Relationship of current with electrode wear along the length (v=5 volts)

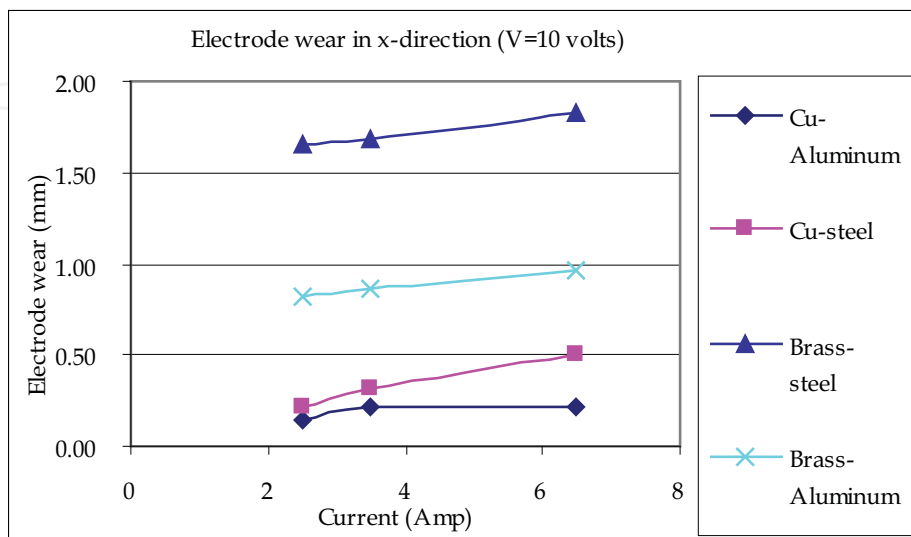


Fig. 8. Relationship of current with electrode wear along the cross-section (v=10 volts)

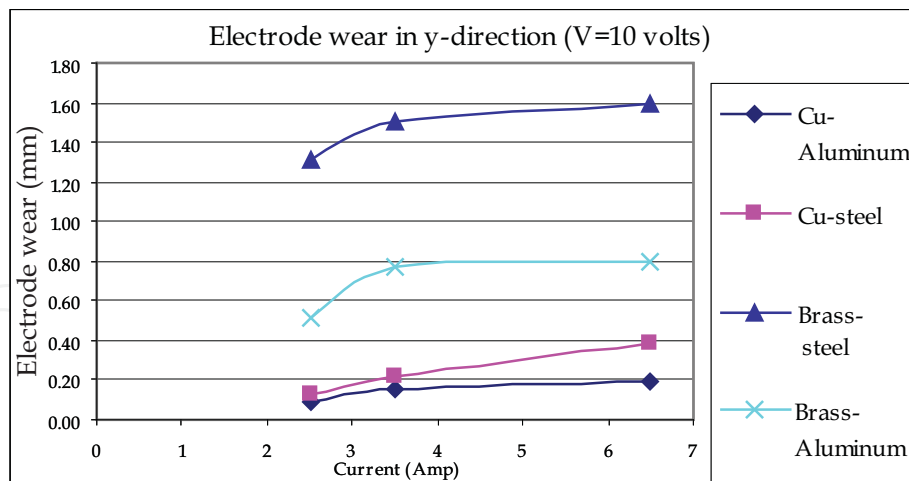
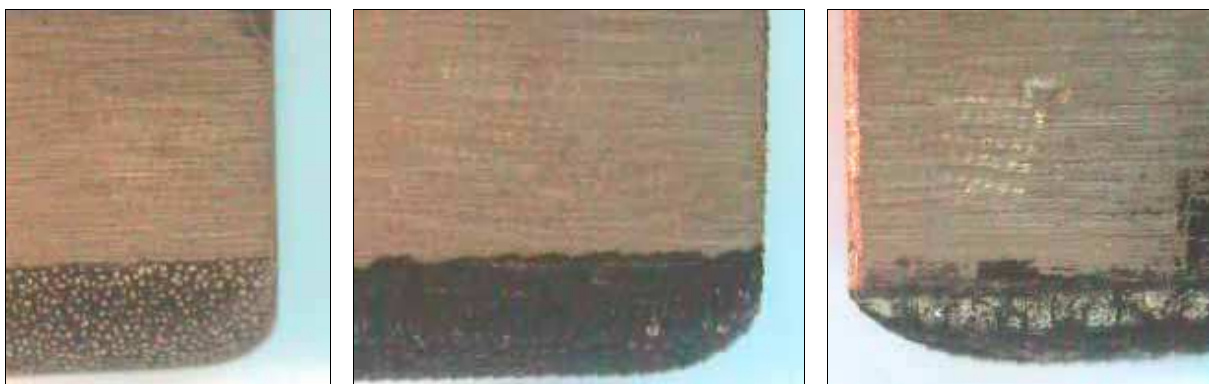


Fig. 9. Relationship of current with electrode wear along the length ( $v=10$  volts)

compared to that in y-direction. This results more wear of electrodes in x-direction compared to that in y-direction. For the same reason it can be expected that that an electrode of a smaller cross-section permits poor heat transfer in x-direction and will undergo more wear compared to that of a larger cross-section. Fig. 10 clearly shows that electrode wear along the cross-section of the electrode is higher compared to the same along its length during machining of aluminum using brass electrodes.



(a) current: 2.5 amps

(b) current: 3.5 amps

(c) current: 6.5 amps

Fig. 10. Wear of brass electrodes; electrode – brass, workpiece – aluminum

Results of the experiments show that copper electrodes undergo less wear compared to brass electrodes. For example, during machining of steel at a current of 3.5 amps and a voltage of 5 volts, the wear of copper electrode is 0.29 mm in x-direction, whereas the same for brass electrode is 1.5 mm (Fig. 6). This is due to the fact that the thermal conductivity of copper (391 W/ m-K) is almost 2.5 times higher than that of brass (159 W/ m-K). This facilitates rapid heat transfer through the body of copper electrodes compared to brass electrodes. It can also be noted that melting point of copper (1083°) is higher to that of brass (990°) that causes less melting and wear of copper electrodes.

From Fig. 6 to Fig. 9 it can also be observed that during machining of steel both the copper and the brass electrodes undergo more wear compared to the same during machining of aluminum. It can be mentioned that thermal conductivity of aluminum (227 W/ m-K) is almost four times to that of steel (51.9 W/ m-K). As a result the heat generated during each

spark is easily absorbed by aluminum compared to that absorbed by steel. This causes less wear of electrodes during machining of aluminum compared to the same during machining of steel. For example, during machining of steel with brass electrodes at a current of 6.5 amps and a voltage of 10 volts electrode wear in y-direction is 1.6 mm, while the same is 0.8 mm during machining of aluminum (Fig. 9).

#### 4.2 Wear ratio

Wear ratio ( $WR$ ) is calculated as the ratio of the material removed from the work to the material removed from the electrode. It can be expressed as follows:

$$WR = \frac{\text{volume of material removed from the electrode}}{\text{volume of material removed from the workpiece}} \times 100\%$$

$$WR = \frac{EVB - EWA}{WPVB - WPWA} \times 100\%$$

where  $EVB$  and  $EWA$  are the volumes of the workpiece before and after machining.

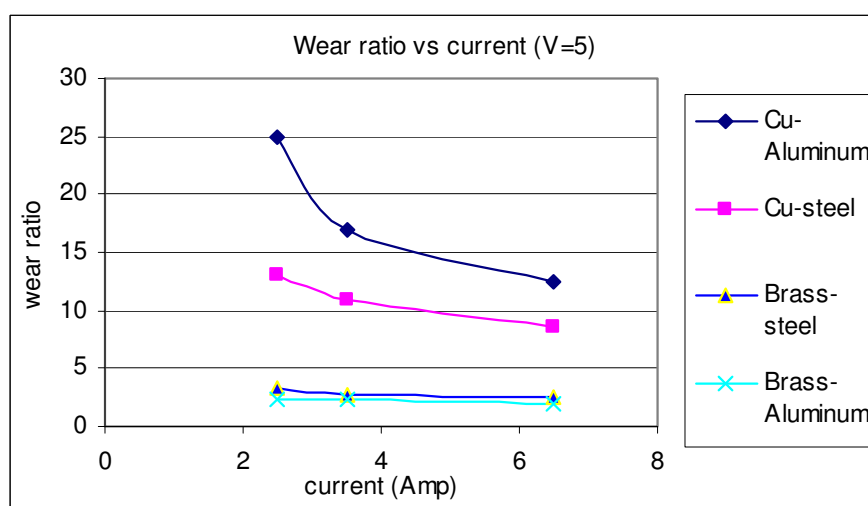


Fig. 11. Relationship of current with wear ratio ( $v=5$  volts)

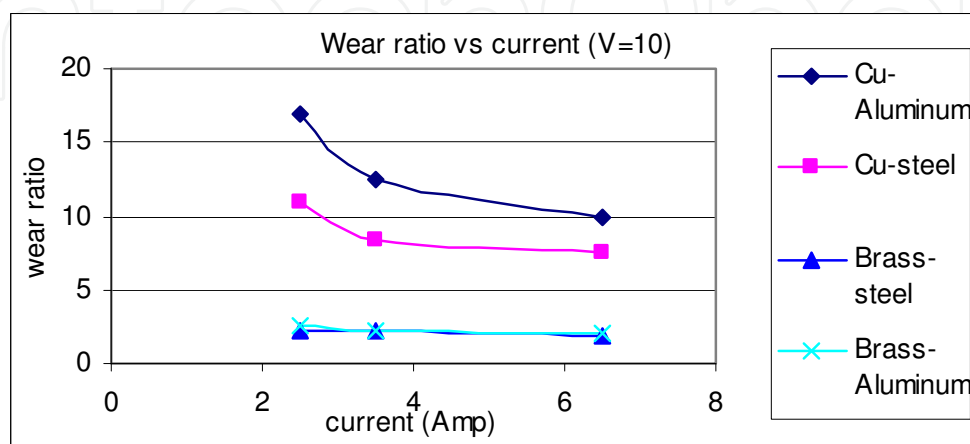


Fig. 12. Relationship of current with wear ratio ( $v=10$  volts)

Fig. 11 and Fig. 12 illustrate the relationship of  $WR$  with current and voltage. It is obvious from the figures that  $WR$  decreases with increase in current. That means, though a higher current causes more removal of work material and the electrode, but comparatively more material is removed from the electrode. At a higher current a stronger spark is generated producing more heat. The size of the workpiece is massive and heat is easily dissipated through it. But since the electrode is a smaller one, heat is accumulated in it resulting high temperature and consequently high  $EW$ .

It can also be observed that  $WR$  is higher at a lower voltage (Fig. 11) compared to that at a higher voltage (Fig. 12). Highest  $WR$  of 25.00 was found during machining of aluminum using a copper electrode at a current of 2.5 amps and a voltage of 5 volts. The total heat generated during a spark is absorbed by the workpiece, electrode, dielectric fluid and the machine parts. It is desirable that most of the heat should be absorbed by the work material, while the least quantity of heat should be absorbed by the electrode. High thermal conductivity of copper electrodes facilitates easy heat transfer and its high melting point facilitates low melting of the electrode material. At the same time, high thermal conductivity of aluminum facilitates easy heat absorption and its low melting temperature facilitates fast removal of work material. These factors result the highest  $WR$  during machining of aluminum using a copper electrode. The lowest  $WR$  of 2.00 was found during machining of aluminum using brass electrodes at a current of 6.5 A and a voltage of 5 volts. Thermal conductivity of brass is only 1.4 times higher than that of the aluminum workpiece and its melting point is approximately 1.5 times higher than that of aluminum. As a result, material removal from the aluminum workpiece is comparatively low and the material removed from the electrode is comparatively high. Therefore, the  $WR$  is only 2.00. From Fig. 11 and Fig. 12 it can be concluded that in order of high to low  $WR$  of electrode-work pair are: copper-aluminum, copper-steel, brass-steel and brass-aluminum.

#### 4.3 Material removal rate

The mechanism of material removal in  $EDM$  is a sudden violent splash of the molten material coinciding with the collapse of the plasma channel. As soon as the spark collapses and the hydrostatic pressure of the arc is released and dielectric rushes back to fill the void, the pressurized molten metal splatters from the workpiece surface leaving a crater on the surface and some splattered fragments around the crater (Shuvra et al, 2003). Material removal mechanism can also be explained in terms of the migration of material elements between the workpiece and electrode. This could take place in the form of elements diffusing from the electrode to the workpiece and vice-versa.

The use of CNC in  $EDM$  has helped to explore the possibility of using alternative methods of tooling to improve the  $MRR$ .  $EDM$  is commonly used for producing complex and deep 3-D shaped cavity in hard materials which necessitate the use of 3-D profile electrodes, which are costly and time-consuming to manufacture for the sparking process. However, in order to produce a complex shape a lot of experimental works have been performed with different types of electrode configurations to generating different path movement on workpiece surfaces by means of controlling the electrode motion.

Flushing pressure has a considerable effect on  $MRR$  and  $EW$ . When the dielectric fluid is forced at low velocity into the spark gap, short-circuiting becomes less pronounced as a result of the accumulated particles. This helps in improving the efficiency and thereby

increases  $MRR$ . Higher flushing pressure hinders the formation of ionized bridges across the gap and results in higher ignition delay and decrease discharge energy and reduces  $MRR$ . It was found by many researchers that the influential machining factors on  $MRR$  are the current intensity and voltage.

Usually  $EDM$  is carried out by electrical sparks between the electrode and the workpiece using a single discharge for each electrical pulse. Some researchers have carried out experiments using a multi-electrode discharging system, delivering additional discharge simultaneously from a corresponding electrode connected serially. The design of electrode was based on the concept of dividing an electrode into multiple electrodes, which are electrically insulated. The energy efficiency were claimed to be better than the conventional  $EDM$  without any significant difference in work surface finish.

Material removal rate is expressed as the ratio of the difference in volume of the workpiece before and after machining to the machining time, i.e.:

$$MRR = \frac{\text{volume of material removed from the workpiece}}{\text{machining time}}$$

$$MRR = \frac{WPVB - WPWA}{MT}$$

where  $WPVB$  and  $WPWA$  are the volumes of the workpiece before and after machining and  $MT$  is the machining time.

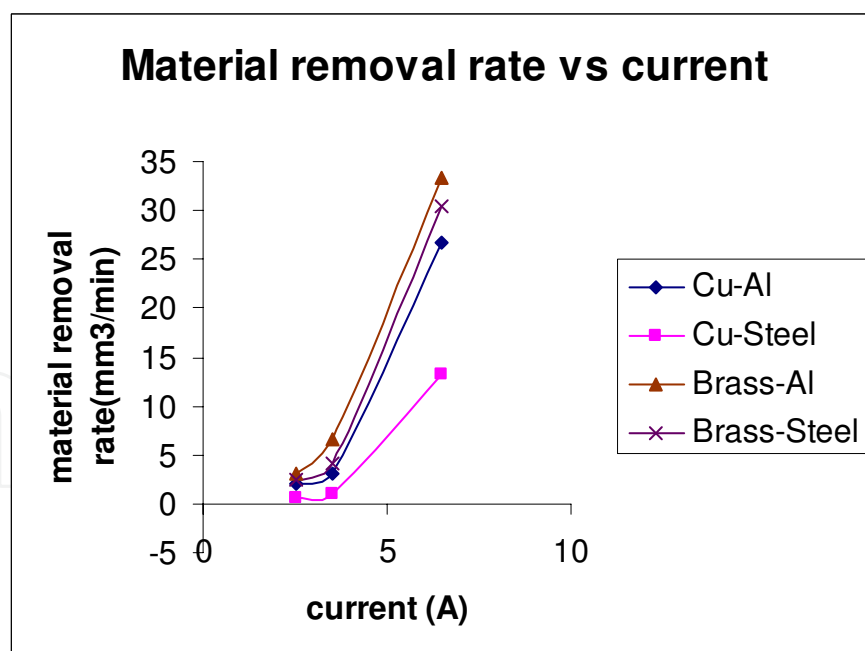


Fig. 13. Relationship between current and MRR

Relationship of  $MRR$  with current during machining of aluminum and steel using brass and copper electrodes are illustrated in Fig. 13. It is to be noted that at a low current  $MRR$  is very low, but with increase in current  $MRR$  increases sharply. At a low current, a small quantity of heat is generated and a substantial portion of it is absorbed by the surroundings and the

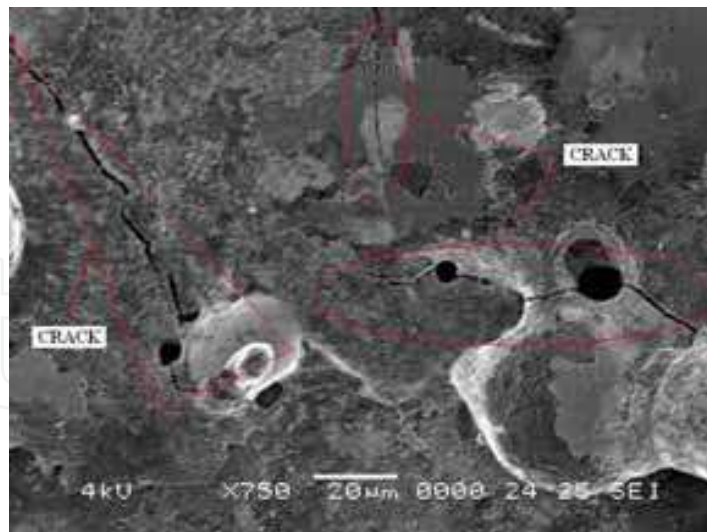
machine components and the left of it is utilized in melting and vaporizing the work material. But as the current is increased, a stronger spark with higher energy is produced, more heat is generated and a substantial quantity of heat is utilized in material removal. However, the highest material removal rate was observed during machining of aluminum using copper electrodes. Comparatively low thermal conductivity of brass as an electrode material doesn't allow absorbing much of the heat energy and most of the heat is utilized in removal of material from aluminum workpiece of low melting point. But during machining of steel using copper electrodes, comparatively smaller quantity of heat is absorbed by the work material due to its low thermal conductivity. As a result *MRR* becomes very low.

#### 4.4 Micro cracks

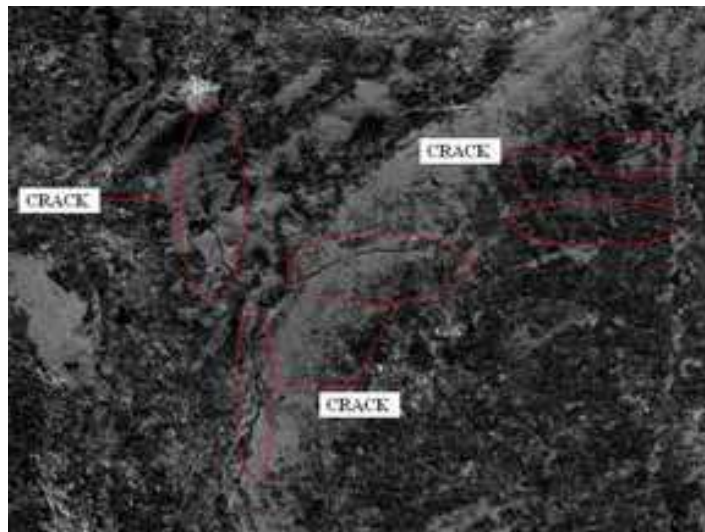
During the spark discharge in *EDM* the temperature is usually in the range of 8,000°C to 20,000°C. After the spark the work surface is immediately cooled rapidly by the dielectric fluid. Repeated heating to a very high temperature followed by rapid cooling develops micro-cracks on the work surface. Micro-cracks on the work surface are a major problem in *EDM*. They strongly influence on the fatigue strength of the part machined by *EDM*. Micro-cracks in the surface and loose grains in the subsurface resulted from thermal shock causes surface damage and leads to degradation of both strength and reliability. Comparing the SEM images in Fig. 14 it can be observed that more micro-cracks were formed during *EDM* with a higher current of 6.5 Amp as shown in Fig. 14 (a) compared to that with a low current of 2.5 Amp as illustrated in Fig. 14 (b). More heat is developed during *EDM* at a higher current heating the work surface to a higher temperature followed by rapid cooling. As a result more micro-cracks are found at a higher current. A larger  $t_{on}$  results more cracks as it can be observed comparing the Figs. 14 (c) and 14 (d). However, it was suggested by Lee & Tai, 2003 that when the pulse voltage is maintained at a constant value of 120 V, it is possible to avoid the formation of cracks if machining is carried out with a current in the range of 12-16 A together with pulse duration of 6-9  $\mu$ s.

#### 4.5 Recast layer

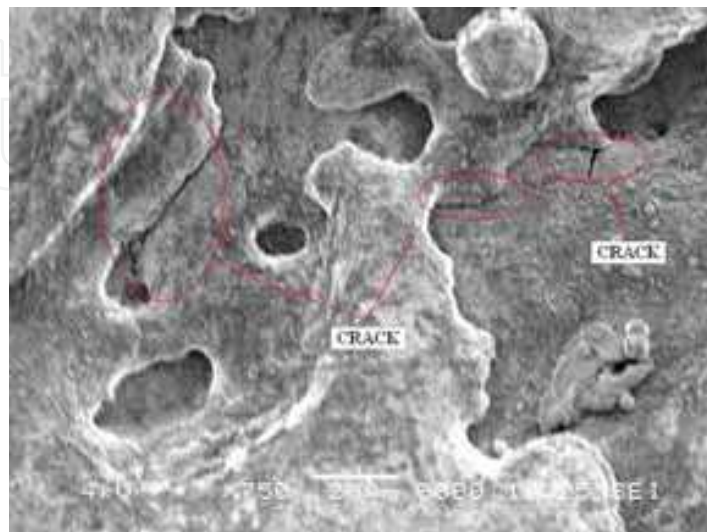
There are three layers created on the top of the base metal which are spattered *EDM* surface layer, recast layer and Heat Affected Zone (*HAZ*). Recast layer consists of dielectric fluid, molten electrode and molten workpiece that are melted during *EDM* machining and solidified. Usually recast layer has a higher hardness when compared to the base metal. The recast layer is also known as white layer because it often appears as a bright white layer in a sectional view under magnification. It occurs as the second layer under the spattered *EDM* surface layer. This layer is formed by the un-expelled molten metal solidifying in the crater. The recast layer is usually very thin and it can be removed by finishing operations. Recast layer can cause problems in some applications due to stress cracking or premature failure. Recast structure greatly affects die fatigue strength and shortens its service life. This is because the recast layers have micro-cracks and discharge craters that cause bad surface quality. *HAZ* consists of two layers: a hardened layer and the annealed layer. The depth of the hardened layer depends on the machining conditions. Usually the depth is 0.002mm for finish cut and 0.012 mm for rough cut. Below the hardened layer there is a layer which was cooled slowly and as a result, the layer is annealed. Its hardness is 2 to 5 points below the same of the base metal. Its thickness may be 0.05mm for finish cut and 0.2mm for rough cut.



(a)  $I=6.5$  Amp;  $t_{on}=10$   $\mu$ s



(b)  $I=2.5$  Amp;  $t_{on}=10$   $\mu$ s



(c)  $I=2.5$  Amp;  $t_{on}=10$   $\mu$ s

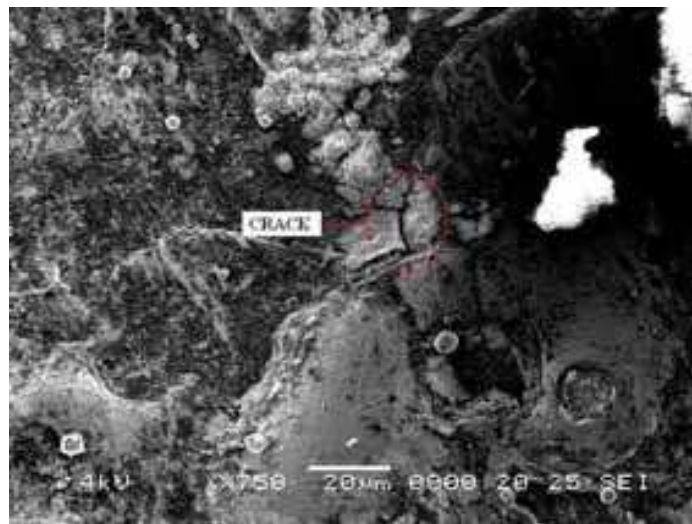
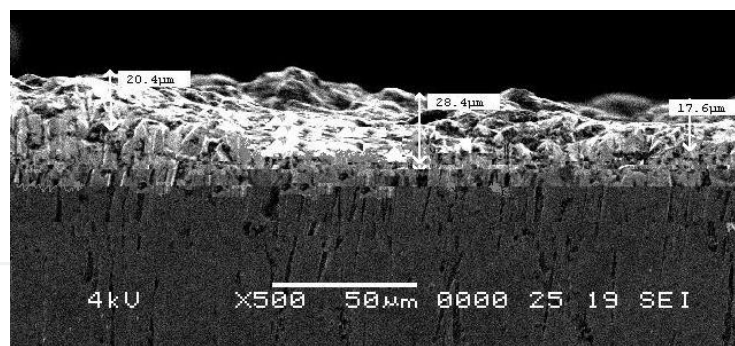
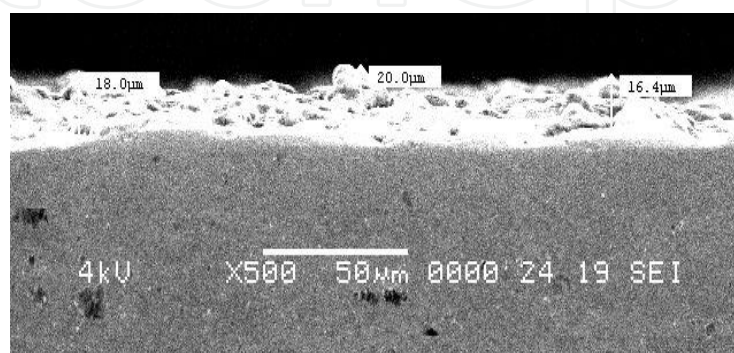
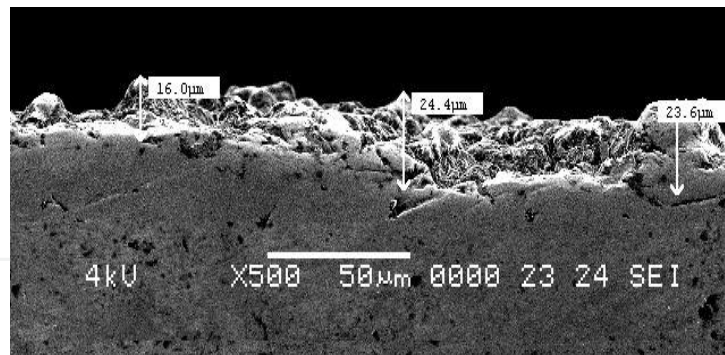
(d)  $I=2.5$  Amp;  $t_{on}=3$   $\mu$ s

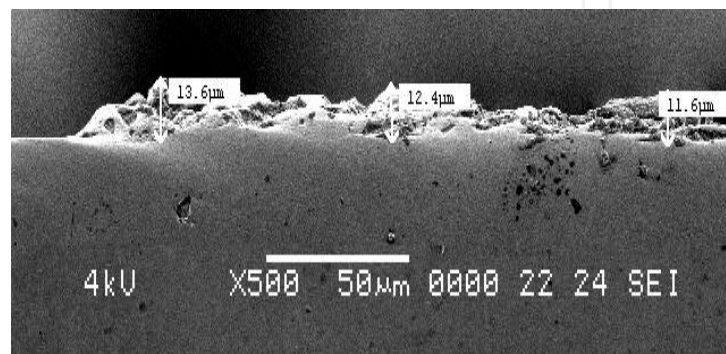
Fig. 14. Influence of current and pulse-on time on micro cracks

As stated above, a higher current and a higher pulse-on time produce a spark with more energy, melt more materials from the workpiece and the electrode. Consequently higher thickness of recast layer is found at a current of 6.5 Amp, Fig. 15 (a) compared to that at a current of 2.5 Amp, Fig. 15 (b). Similarly, thickness of the recast layer was found to be at a higher pulse-on time, Fig. 15 (c) compared to that at a shorter pulse-on time, Fig. 15 (d). Hwa-Teng Lee et al., 2004 also stated that  $R_a$  and average white layer thickness tend to increase at higher values of pulse current and  $t_{on}$ . However, they found that for extended pulse-on duration  $MRR$ ,  $R_a$  and crack density all decrease.

(a)  $t_{av}$  22.1  $\mu$ m:  $I= 6.5$  Amp;  $t_{on}=10\mu$ s(b)  $t_{av}$  18.1  $\mu$ m:  $I= 2.5$  Amp;  $t_{on}=10$   $\mu$ s



(c)  $t_{av}$  21.3  $\mu\text{m}$ ;  $I= 2.5$  Amp;  $t_{on}=10$   $\mu\text{s}$



(d)  $t_{av}$  12.5  $\mu\text{m}$ ;  $I= 2.5$  Amp;  $t_{on}=1.5$   $\mu\text{s}$

Fig. 15. Thickness of recast layer at different machining conditions

## 5. Conclusion

From the above discussions the following conclusions can be drawn:

1. Electrodes undergo more wear along its cross-section compared to that along its length.
2. Electrode wear increases with increase in current and voltage. Wear of copper electrodes is less than that of brass electrodes. This is due to the higher thermal conductivity and melting point of copper compared to those of brass.
3. During machining of mild steel, electrodes undergo more wear than during machining of aluminum. This is due to the fact that thermal conductivity of aluminum is higher to that of mild steel which causes comparatively more heat energy to dissipate into the electrode during machining of mild steel.
4. Wear ratio decreases with increase in current, but decreases with increase in gap voltage. The highest wear ratio was found during machining of aluminum using a copper electrode.
5. MRR increases sharply with increase in current. In the present study, highest MRR was obtained during machining of aluminum using a brass electrode.
6. Micro cracks are found on the machined surface. The tendency of formation of micro cracks increases during EDM with a higher current and larger pulse-on time.
7. A recast layer was found on the machined surface which consists of the molten materials from the workpiece and the electrode that could not be flushed away completely by the dielectric fluid. A thicker layer of recast layer was formed on the work surface machined with a higher current and pulse-on time.

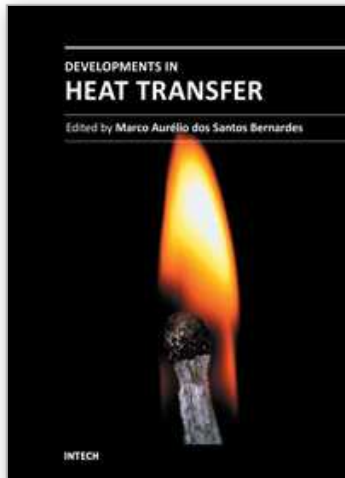
## 6. Acknowledgement

The author of this work is indebted to the Research Management Center, International Islamic University Malaysia (IIUM) for its continuous help during the research work. Also, the author likes to appreciate the help of the staff and the technicians of the Department of Manufacturing and Materials Engineering, International Islamic University Malaysia.

## 7. References

- Bleys, P.; Kruth, P. & Lauwers, B. (2004). Sensing and compensation of tool wear in milling EDM. *Journal of Materials Processing Technology*, vol.149, No.1-3, pp. 139-146, ISSN 0924-0136
- Bulent, E.; Erman, A. & Abdulkadir E. (2006). A semi-empirical approach for residual stresses in electric discharge machining (EDM). *International Journal of Machine Tool & Manufacture*. Vol.46, pp. 858-865, ISSN 0890-6955
- Dibitonto, D.; Eubank, T.; Patel, R. & Barrufet, A. (1989). Theoretical models of the electro discharge machining process—a simple cathode erosion model. *Journal of Applied Physics*, vol.69, pp. 4095-4103, ISSN 0021-8979
- Ghosh, A. & Mallik, K. (1991). Electrical Discharge Machining, In: *Manufacturing Science*, 383-403, Affiliated East- West Press Private Limited, ISBN 81-85095-85-X, New Delhi, India.
- Ho, H. & Newman, T. (2003). State of the art electrical discharge machining (EDM). *International Journal of Machine Tools and Manufacture*, vol.43, No.13, pp. 1287-1300, ISSN 0890-6955
- Hu, F. Zhou, C. & Bao, W. (2008). Material removal and surface damage in EDM of Ti<sub>3</sub>SiC<sub>2</sub> ceramic. *Ceramics International*, vol.34, issue 3, pp. 537-541, ISSN 0272-8842
- Hwa-Teng, L.; Fu-Chuan Hsu & Tzu-Yao, T. (2004). Study of surface integrity using the small area EDM process with a copper-tungsten electrode, *Materials Science and Engineering A*, vol. 364, issues 1-2, pp. 346-356, ISSN 0025-5416
- Kalpakjian, S. Schmid, R. (2001). Electrical-discharge machining, in: *Manufacturing Engineering and Technology*, 6<sup>th</sup> edition, Prentice Hall, 769-774, Singapore
- Khan, A. & Mridha, S. (2006). Performance of copper and aluminum electrode during EDM of stainless steel and carbide. *International Journal of Manufacturing and Production*, vol. 7, No.1, pp. 1-7, ISSN 0793-6648
- Khanra, K.; Sarker, R.; Bhattacharya, B.; Pathak, C. & Godkhindi, M. (2007). Performance of ZrB<sub>2</sub>-Cu composite as an EDM electrode. *Journal of Materials Processing Technology*, vol.183, No.1, pp. 122-126, ISSN 0924-0136
- Kunieda, M. & Kobayashi, T. (2004). Clarifying mechanism of determining tool electrode wear ratio in EDM using spectroscopic measurement of vapor density. *Journal of Materials Processing Technology*, vol.149, No. 1-3, pp. 284-288, ISSN 0924-0136
- Lee, T. & Tai, Y. (2003). Relationship between EDM parameters and surface crack formation. *Journal of Materials Processing Technology*, vol.142, issue 3, pp. 676-683, ISSN 0890-6955
- Marafona, J & Wykes. C. (2000). A new method of optimizing material removal rate using EDM with copper-tungsten electrodes. *International Journal of Machine Tools and Manufacture*, vol.40, pp. 153-164, ISSN 0890-6955
- Marafona, J, & Chousal, G. (2006). A finite element model of EDM based on the Joule effect. *International Journal of Machine Tools & Manufacture*, vol.46, pp. 595-602, ISSN 0890-6955
- Pandey, C. & Jilani, T. (1986). Plasma channel growth and the resolidified layer in EDM. *Precision Engineering*, Vol.8, issue 2, pp. 104-110, ISSN 0141-6359

- Ozgedik, A. & Cogun, C. (2006). An experimental investigation of tool wear in electric discharge machining. *International Journal of Advance Manufacturing Technology*. Vol.27, pp. 488-500, ISSN 0268-3768
- Patel, R.; Barrufet, A.; Eubank, T. & DiBitonto, D. (1989). Theoretical models of the electrical discharge machining process-II: the anode model. *Journal of Applied Physics*, vol.66, pp. 4104-4111, ISSN 0021-8979
- Peter, Fonda.; Zhigang, Wang.; Kazuo, Yamazaki. & Yuji, A. (2007). A fundamental study on Ti-6Al-4V's thermal and electrical properties and their relation to EDM productivity. *Journal of Materials Processing Technology*, doi:10.1016/j.jmatprotec.2007.09.060, ISSN 0924-0136
- Puertas, I.; Luis, J. & Alvarez, L. (2004). Analysis of the influence of EDM parameters on surface quality, MRR and EW of WC-Co. *Journal of Materials Processing Technology*, vol.153-154, No.10, pp. 1026-1032, ISSN 0924-0136
- Ramasawmy, H. & Blunt, L. (2001). 3D surface characterization of electropolished EDMed surface and quantitative assessment of process variables using Taguchi Methodology. *International Journal of Machine Tools and Manufacture*, vol.42, pp. 1129-1133, ISSN 0890-6955
- Salonitis, K.; Stournaras, A.; Stavropoulos, P. & Chryssolouris, G. (2007). Thermal modeling of the material removal rate and surface roughness for die-sinking EDM. *International Journal of Advance Manufacturing Technology*. DOI 10.1007/s00170-007-1327-y, ISSN 0268-3768
- Shuvra, D.; Mathias, K. & Klocke, F. (2003). EDM simulation: finite element-based calculation of deformation, microstructure and residual stresses. *Journal of Materials Processing Technology*, vol.142, pp. 434-451, ISSN 0924-0136
- Tariq, S. & Pandey, C. (1984). Experimental investigation into the performance of water as dielectric in EDM, *International Journal of Machine Tool Design and Research*, vol.24, pp. 31-43, ISSN 0020-7357
- Thomas, N.; Shreyes, M.; Thomas, W.; Rosa, T. & Laura, R. (2009). Investigation of the effect of process parameters on the formation and characteristics of recast layer in wire-EDM of Inconel 718. *Materials Science and Engineering: A*, vol.513-514, pp. 208-215, ISSN 0025-5416
- Vinod, Y.; Vijay, K. & Prakash, M. (2002). Thermal stresses due to electrical discharge machining, *International Journal of Machine Tools & Manufacture*. Vol.42, pp. 877-888, ISSN 0890-6955
- Wang, J. & Tsai, M. (2001a) Semi-empirical model on work removal and tool wear in electrical discharge machining. *Journal of materials processing technology*, vol.114, No.4, pp. 1-17, ISSN 0924-0136
- Wang, J. & Tsai, M. (2001b). Semi-empirical model of surface finish on electrical discharge machining. *International Journal of Machine Tools and Manufacture*, vol.41, pp. 1455-1477, ISSN 0890-6955
- Yan, H.; Tsai, C. & Huang, Y. (2005). The effect of EDM of a dielectric of a urea solution in water on modifying the surface of titanium. *International Journal of Machine Tools and Manufacture*, vol. 45, No.2, pp. 194-200, ISSN 0890-6955
- Zarepour, H.; Tehrani, A.; Karim, D. & Amini, S. (2007). Statistical analysis on electrode wear in EDM of tool steel DIN 1.2714 used in forging dies. *Journal of Material Processing Technology*, vol.187-188, pp. 711-714, ISSN 0924-0136
- Zaw, M.; Fuh, H.; Nee, C. & Lu, L. (1999). Fabrication of a new EDM electrode material using sintering techniques. *Journal of Materials Processing Technology*, vol.89-90, pp. 182-186, ISSN 0924-0136



## **Developments in Heat Transfer**

Edited by Dr. Marco Aurelio Dos Santos Bernardes

ISBN 978-953-307-569-3

Hard cover, 688 pages

**Publisher** InTech

**Published online** 15, September, 2011

**Published in print edition** September, 2011

This book comprises heat transfer fundamental concepts and modes (specifically conduction, convection and radiation), bioheat, entransy theory development, micro heat transfer, high temperature applications, turbulent shear flows, mass transfer, heat pipes, design optimization, medical therapies, fiber-optics, heat transfer in surfactant solutions, landmine detection, heat exchangers, radiant floor, packed bed thermal storage systems, inverse space marching method, heat transfer in short slot ducts, freezing and drying mechanisms, variable property effects in heat transfer, heat transfer in electronics and process industries, fission-track thermochronology, combustion, heat transfer in liquid metal flows, human comfort in underground mining, heat transfer on electrical discharge machining and mixing convection. The experimental and theoretical investigations, assessment and enhancement techniques illustrated here aspire to be useful for many researchers, scientists, engineers and graduate students.

### **How to reference**

In order to correctly reference this scholarly work, feel free to copy and paste the following:

Ahsan Ali Khan (2011). Role of Heat Transfer on Process Characteristics During Electrical Discharge Machining, *Developments in Heat Transfer*, Dr. Marco Aurelio Dos Santos Bernardes (Ed.), ISBN: 978-953-307-569-3, InTech, Available from: <http://www.intechopen.com/books/developments-in-heat-transfer/role-of-heat-transfer-on-process-characteristics-during-electrical-discharge-machining>

**INTECH**  
open science | open minds

### **InTech Europe**

University Campus STeP Ri  
Slavka Krautzeka 83/A  
51000 Rijeka, Croatia  
Phone: +385 (51) 770 447  
Fax: +385 (51) 686 166  
[www.intechopen.com](http://www.intechopen.com)

### **InTech China**

Unit 405, Office Block, Hotel Equatorial Shanghai  
No.65, Yan An Road (West), Shanghai, 200040, China  
中国上海市延安西路65号上海国际贵都大饭店办公楼405单元  
Phone: +86-21-62489820  
Fax: +86-21-62489821

© 2011 The Author(s). Licensee IntechOpen. This chapter is distributed under the terms of the [Creative Commons Attribution-NonCommercial-ShareAlike-3.0 License](#), which permits use, distribution and reproduction for non-commercial purposes, provided the original is properly cited and derivative works building on this content are distributed under the same license.

IntechOpen

IntechOpen